Materials Research. 2019; 22(5): e20180534
DOI: http://dx.doi.org/10.1590/1980-5373-MR-2018-0534

Design of Three-Layer Antireflection Coating for High Reflection Index Lead Chalcogenide

Muhammad Mansoor[a]*, Abubakar[a], Saba Zaman[a], Liaqat Ali[a,b], Shaheed Khan[a]

[a]*Institute of Industrial Control Systems, Rawalpindi-PAKISTAN*
[b]*Department of Metallurgical Engineering & Materials Science, University of Engineering & Technology, Lahore, Pakistan*

Received: July 30, 2018; Revised: September 28, 2019; Accepted: October 10, 2019

Antireflection coatings (ARC), not only reduce the reflection of the incident radiation but also protect the surface from environmental degradations. In present study, three- layer design was theoretically calculated and experimentally realized on the surface of lead chalcogenide, which had high refractive characteristics. First the theoretical designs of three- layers of different dielectric materials (i.e., ZnSe, SnO_2, SiO and MgF_2) were simulated using optical matrix approach. Subsequently, the developed designs were experimentally produced on lead sulfide thin films using thermal evaporation technique. The efficiency of the designs was evaluated for 1500-2400 nm spectral range and found that the design comprising ZnSe-SiO-MgF_2 had 23% better performance than ZnSe-SnO_2-MgF_2, besides consistent coating adhesion and morphology. The difference between theoretical and experimental results was less than 10 and 16 % for ZnSe-SiO-MgF_2 and ZnSe-SnO_2-MgF_2, respectively.

Keywords: *Three-layer antireflection coating; Theoretical design; Thermal evaporation; Experimental coatings; Dielectric materials.*

1. Introduction

As fabricated optical systems are always accompanied by optical losses in terms of reflectance, absorbance and scattering; of which, reflectance could be the major source[1]. It is customary to use antireflection (AR) coatings to reduce the losses, however using AR coatings is not a hackneyed process due to its limitations of diverse optical materials need, optimum films thickness, and structure/ defects of the film to be realized. There are various forms of AR coatings: a single- layer AR coating may provide a virtual zero reflectance at one selected wavelength, a double- or three- layer AR coating may provide virtual zero reflectance at two or three wavelengths, and so on to multi- layer AR coatings[2]. Requirements to develop newer AR coatings has been significantly increased during past few years, which is more prudent and reliable due to the availability of advanced data acquisition and computation through software based applications[3]. Potential applications of the AR coatings include spectacles, binocular lenses, solar cells, optical filters, infrared and laser diodes[4]. These coatings perform complete cancellation of reflectance from the upper and lower interfaces of the films. Despite the fact that numerous recipes have been developed so far, however the research is still going on for the diversity of the materials and applications.

The contemporary development of optoelectronic devices like touchscreens, sensors, and camera lenses, put new requirements on the researchers, including three primary characteristic of the AR coating: i) submicron thickness, ii) least sensitive to the incidence angle and iii) large optical wavelength range [5,6]. The very first approach to address these questions is single-layer AR coating, where the light intensity is calculated reflected by any surface; accordingly a non-absorbing material is required with specific refractive index and thickness. In this approach, a uniform and consistent coating is essential to achieve calculated results. The additional bottle necks of the technique are: narrow or practically single wavelength range and very limited glazing angle response[7]. Alternatively, a popular approach in AR coatings is double layer technique, which has characteristic feature to reduce the reflection for definite wavelength. The technique comprises a top layer, facing the atmosphere, having least possible refractive index, while the bottom layer has the refractive index in ascending order such that the interference conditions should be fulfilled in order to destructively cancel the reflecting waves from the surface of the substrate. The intrinsic limitation of the double layer technique is limited response to the wavelength bands[8].

A more versatile approach to address the issues of AR coatings is deposition of more than two dielectric layers. The technique provides a precise control destructive interference of reflecting spectra hence reduce the overall reflection[9, 10]. The performance of the multilayer AR coating strongly related with the refractive index and thickness of the individual layer. Multilayer AR coatings may facilitate numerous broadband dips in the reflection spectra at different wavelength [11, 12]. Loh et al. used multilayers of porous silica nano films, which resulted in reduction of the reflection of glass down to 1% [13]. Many other researchers have used the techniques for glass and silicon based substrate materials, which have moderate to low refractive indexes[14-16].

*e-mail: malik01677@yahoo.com.

However, fewer workers reported their work on highly reflective substrates. For example, Reddy et al. deposited SnO_2 and ZnO coatings using solution growth and spray pyrolysis technique to reduce the reflectance down to 90%, however their results were optimized for specific short range optical spectra[17].

Due to its toxicity, PbS has little commercial importance, however it is the oldest detector material for the detection of infrared spectra. It functions as photon detector and responds directly to the radiated photons. Usually thin films of PbS are used as detector elements, where their ability to produce photocurrent or vary the electrical resistance is used for the detection. However, the ability to change in electrical resistance is more pronounced, therefore more commonly used in infrared detection. PbS has an intrinsic feature to detect infrared wavelength range of 1000 to 2500 nm at room temperature. This infrared wavelength is known as near-wavelength infrared (NWIR), which is the infrared range emitted by very hot objects[17, 18].

In the present work, two combinations of three- layer AR coatings were theoretically modeled on lead sulfide thin films, which were coated on quartz substrate. In these combinations, first and last layer remained the same i.e., MgF_2 and ZnSe, respectively, whereas the sandwich layer was either SiO or SnO_2. The performance of these coatings was optimized by varying the individual layer thickness for a specific design wavelength, subsequently the modeled coatings were fabricated experimentally. Thermal evaporation technique was used to deposit the films and scanning electron microscopy, atomic force microscopy, x-ray diffraction, and spectrophotometry were used to evaluate the characteristics of the experimental AR coatings. The scope entailed the formation for minimum reflectance in the spectral range of 1400 to 2500 nm, using low cost and easy to evaporate materials.

2. Theoretical Considerations & Numerical Design

The simplest model of antireflection coating may comprise a substrate coated with a single layer, where the magnitude of antireflection is driven by the extent of cancelation of light by upper and lower surface of the coating, which implies; the intensity of reflection from upper and lower surfaces should be equal to attain complete extinction of the reflection[19,20]. In physical implications, the ratio between refractive indexes of air (n_o) and coating (n_1) should be equal to the ratio between n_1 and refractive index of the substrate (n_u):

$$\frac{n_0}{n_1} = \frac{n_1}{n_u} \tag{1}$$

while the physical film thickness (t_j) at design wavelength (λ) would be:

$$n_1.tj = \frac{\lambda}{4} \tag{2}$$

Such a type of antireflection coating will give rise one minimum in reflection profile, however for more minima more layers would be required, which is the fundamental theory of optical matrix approach to develop mathematical models for two-, three- or multi- layer antireflection coatings[21]. Such a mathematical model used to for designing of multilayer antireflection coating is presented in Eq-3, which is the basic expression for the design of n number of layers[22]:

$$\begin{bmatrix} B \\ C \end{bmatrix} = \sum_{j=1}^{N} \begin{bmatrix} \cos\delta j & \left(\frac{i}{nj}\right)\sin\delta j \\ i.\,nj.\sin\delta j & \cos\delta j \end{bmatrix} \begin{bmatrix} 1 \\ n_u \end{bmatrix} \tag{3}$$

where, B and C represent total electrical and magnetic amplitudes of propagating light, respectively. The refractive index of the substrate is η_u and η_j is refractive index of j^{th} layer, where j=1, 2, 3…..N. The δ_j represents the phase thickness of j^{th} layer at λ wavelength and is equal to:

$$\delta j = \frac{2\pi}{\lambda} nj.tj \tag{4}$$

The ratio between B and C represents optical admittance (Y):

$$Y = \frac{C}{B} \tag{5}$$

To calculate the combine reflectance of multiple thin coatings, characteristics matrix of individual coatings is used i.e., Eq-6 represents the characteristics matrix of n number of coatings at design wavelength (λ):

$$M = M_1.M_2.M_3.\ldots\ldots\ldots Mn \tag{6}$$

Therefore, each layer of the thin film is represented by a 2x2 matrix, as follows:

$$Mj = \begin{bmatrix} \cos\delta j & \left(\frac{i}{nj}\right)\sin\delta j \\ i.nj.\sin\delta j & \cos\delta j \end{bmatrix} \tag{7}$$

The coefficient of reflection (r) and corresponding reflectance (R) could be determined using Eq-8 and 9:

$$r = \frac{n_o - Y}{n_o + Y} \tag{8}$$

$$R = r \times r = \begin{bmatrix} n_o - Y \\ n_o + Y \end{bmatrix} \begin{bmatrix} n_o - Y \\ n_o + Y \end{bmatrix} \tag{9}$$

For a three- layer antireflection coating, Eq-3 will become:

$$\begin{bmatrix} B \\ C \end{bmatrix} = \sum_{j=1}^{3} \begin{bmatrix} \cos\delta_1 & \left(\frac{i}{n_1}\right)\sin\delta_1 \\ i.n_1.\sin\delta_1 & \cos\delta_1 \end{bmatrix} \ldots\ldots\ldots\ldots \begin{bmatrix} \cos\delta_3 & \left(\frac{i}{n_3}\right)\sin\delta_3 \\ i.n_3.\sin\delta_3 & \cos\delta_3 \end{bmatrix} \begin{bmatrix} 1 \\ n_u \end{bmatrix} \tag{10}$$

Consequently, for quarter- and half- wave optical thickness coatings, the reflectance at normal incidence will become:

$$Mj\left(\frac{1}{4}\lambda\right)=\begin{bmatrix}0 & \frac{i}{nj}\\ i.nj & 0\end{bmatrix} \quad (11)$$

$$Mj\left(\frac{1}{2}\lambda\right)=\begin{bmatrix}1 & 0\\ 0 & 1\end{bmatrix} \quad (12)$$

To solve the three- layer antireflection design, the reflectance was supposed to be minimum i.e., R≈0. With the supposition, Eqs- 9 to 12 were used to determine required refractive index of each layer:

$$n_1^4 = n_0^3 n_s \text{ thus, } n_1 = 1.41 \quad (13)$$

$$n_2^4 = n_0^2 n_s^2 \text{ thus, } n_2 = 1.98 \quad (14)$$

$$n_3^4 = n_0 n_s^3 \text{ thus, } n_3 = 2.79 \quad (15)$$

where, n_0=1 for air and n_s=3.92 for lead sulfide between 1000 to 2500 nm spectral range.

According to Eq-13, the required refractive index was 1.41 for top layer; therefore, MgF_2 was selected, which is a dielectric material having 1.38 index of reflection. For the center layer, the calculated value of the refractive index was 1.98, as mentioned in Eq-14. To meet the requirement two different materials i.e., SiO (n=1.95) and SnO_2 (n=2.01) were selected. Finally, ZnSe was selected for the third layer; whose refractive index (n=2.89) is close to the calculated in Eq-15.

The reflectivity of lead sulfide substrate coated with two different combinations of three-layer antireflection coatings were simulated using MetLab-R2010 software. The two combinations of the three-layer antireflection coatings were comprised of MgF_2-SiO-ZnSe and MgF_2-SnO_2-ZnSe. The simulation of the refractivity was effectuated in the spectral range of 1500-2400 nm. The parameters used for the simulation included: optical thickness and refractive index of each layer.

3. Experimental Coatings

3.1 Lead sulfide coating

Thin films of lead sulfide were coated on the quartz substrates using chemical bath deposition (CBD) method. Prior to the deposition, the substrates were treated in 50% solution of hydrochloric acid and then immersed in concentrated sulfuric acid for 2 hours, subsequently, the substrates were washed in distilled water and dried at 80 °C. The chemical bath was prepared using solutions of lead acetate (the Pb^{2+} ion source), thiourea (the S^{2-} ion source) and hydrazine hydrate in de-ionized water at a proportion of 1:1:5 (mol./L), respectively. The cleaned substrates were placed horizontally in the beaker containing the reactant solutions. Temperature was kept at 95 °C, while the bath remained stagnant after initial stirring for five minutes. Coating was carried out for 30 minutes; afterwards, the coated substrates were thoroughly washed with boiling water and dried in oven at 65-70 °C for one hour. The film thickness was measured using density method and the structural properties were evaluated by X-ray diffraction (XRD) analysis using CuKα radiation. A scanning electron microscope (SEM) and atomic force microscope (AFM) were used to study the surface morphologies and roughness of the deposited films.

3.2 AR coating

The lead sulfide coated quartz substrates were, subsequently used for deposition of antireflection coatings. Two combinations of the three coating materials were deposited such that ZnSe was the first coating on the lead sulfide substrate, second was SiO or SnO_2 sandwich coating, while last coating was MgF_2; interfacing with air.

The used materials were of coating grade specifications with high purity. A thermal evaporation coating unit was used to deposit the coating materials. The thermal evaporation technique has added benefit of low process cost when compared with other coating processes besides its availability. During the coating process a vacuum level of 5_X10^{-6} mbar was maintained, while the substrate temperature was kept at 250 °C. Tungsten and molybdenum boats were used as evaporation source for SiO/SnO_2 and ZnSe/MgF_2, respectively. The coating thickness was monitored using an in-situ thickness meter. The substrates were revolved in planetary direction to attain uniform film deposition.

Additionally, precautionary measures were taken during evaporation process to minimize spitting and splashing of the coating materials. For which, heating current was increased slowly, accompanying hold times at various values of the current, until the start of the evaporation. Afterwards, the current was adjusted to desired evaporation rate (2 Å/sec.). Once the desired evaporation rate was achieved; the mechanical shutter was opened to start deposition on the substrates. All the three coating materials were placed in separate boats in the vacuum chamber and individual film was deposited according to the predetermined thickness and sequence.

After the deposition process, the coated substrates were stress relieved at 200 °C for three hours under vacuum. The cooling of the substrates was carried out at the rate of 2 °C/min. till 90 °C, afterwards the heating was turned off and the substrates were cooled to room temperature in the chamber under vacuum.

The coated substrates were subjected to Shimadzu UV-3600A spectrophotometer for the determination of reflection spectra in the range of 1400-2500 nm. The substrates were also studied using scanning electron microscope in secondary electron imaging mode with objective aperture-2.

4. Results and Discussion

Results of simulated reflection spectra are shown in Figure 1, where the two discrete reflection spectra are calculated at the design wavelength of 2000 nm and plotted on a spectral range of 1500-2400 nm. The topmost dotted horizontal line represents the theoretical reflected spectrum of lead sulfide. Remaining two-line represent the antireflection coatings of the combinations: MgF_2-SiO-ZnSe and MgF_2-SnO_2-ZnSe, where MgF_2 being the layer interfacing with air and ZnSe being layer adjacent to lead sulfide.

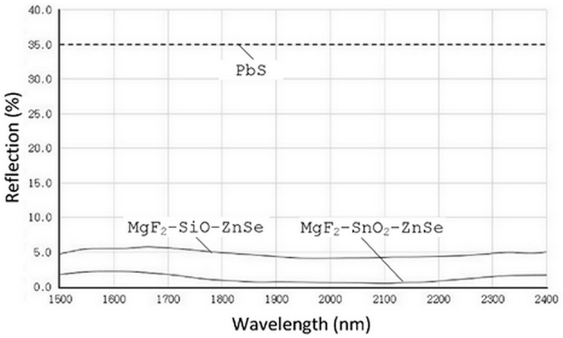

Figure 1. Superimposed reflection spectra generated using theoretical models.

The calculated physical thickness for each layer of the two combinations of the three- layers antireflection coatings are given in Table 1.

During numerical investigations and modeling, it was elaborated that the three layers may have refractive indexes of 1.41, 1.98 and 2.79; starting from air interface to the substrate. Therefore, MgF_2 and ZnSe were selected as air and substrate interface material, respectively, while for the mid-layer two different materials were selected: SiO having the refractive index just below of calculated layer and SnO_2 having the refractive index just above.

In Figure 1, it could be seen that both the combinations of three-layer coatings exhibited appreciably lower reflections than uncoated lead sulfide surface. The first combination of the layers comprising MgF_2-SiO-ZnSe had minima of 4% reflection between 1950 to 2150 nm, whereas the second combination of MgF_2-SnO_2-ZnSe had the minima range from 1820 to 2150 nm with less than 1% reflection.

Lead sulfide thin films deposited by CBD method had a thickness of 750nm, determined by density weight method. While XRD scan, shown in Figure 2, revealed that the structure was polycrystalline face-centered cubic with the space group Fm3m having structural parameter of 5.986 Å, which were in closed tolerance to the standard specifications of PCPDF card No: 781901.

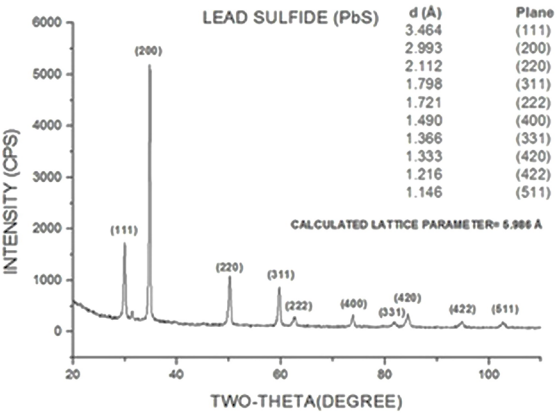

Figure 2. XRD scan of lead sulfide thin film.

The morphology of the coated film was studied using SEM (Figure 3a), where facets of lead sulfide crystals could be seen. These facets have uniform size distribution on the whole spread, however, few film defects and discontinuities were also present. The surface roughness profile was determined using an atomic force microscope and found that average surface roughness was 398 nm (Figure 3b). The grain size of the lead sulfide thin film was also calculated from AFM micrographs and found 400±6 nm.

SEM investigations were carried out on the lead sulfide thin film substrates, after the deposition of two combinations of the three- layers antireflection coatings, separately. The representative micrographs are shown in Figure 4. The general morphology of the coatings appeared comparable to each other, however, the grain boundaries of MgF_2-SnO_2-ZnSe coating were discernable and uniformly present throughout the specimen. At higher magnification, these boundaries were accompanied by mud cracking type features, which attributed to excessive shrinkage. Whereas, the MgF_2-SiO-ZnSe coating was free from such types of cracking.

Table 1. Calculated physical thicknesses of the two combinations of three- layer antireflection coatings along with different properties.

Combination	Order of coating	Top Layer	Middle Layer	Bottom Layer
I	Material	MgF_2	SiO	ZnSe
	Thickness (nm)	173.01	312.50	362.32
	Refractive Index	1.38	1.95	2.89
II	Material	MgF_2	SnO_2	ZnSe
	Thickness (nm)	173.01	250.00	362.32
	Refractive Index	1.38	2.01	2.89

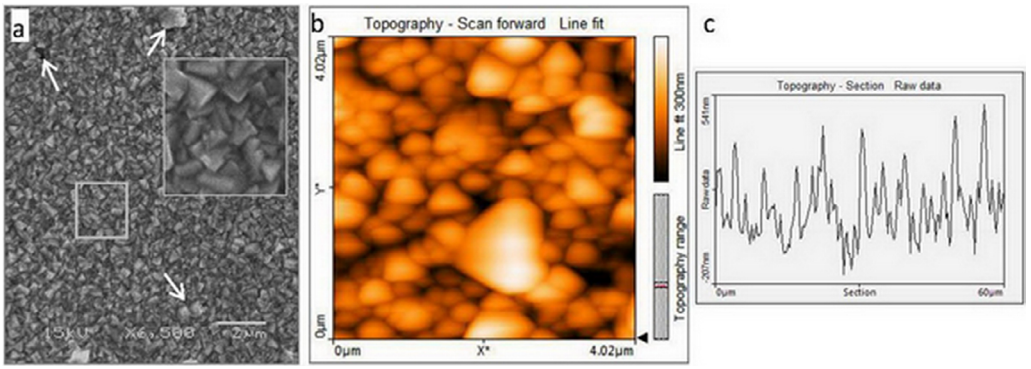

Figure 3. a) Microstructural features of the lead sulfide thin film, inset is at 25000x magnification of the selected area. Arrows are indicating defects in the film. b) AFM micrograph and c) the surface roughness profile (S_a).

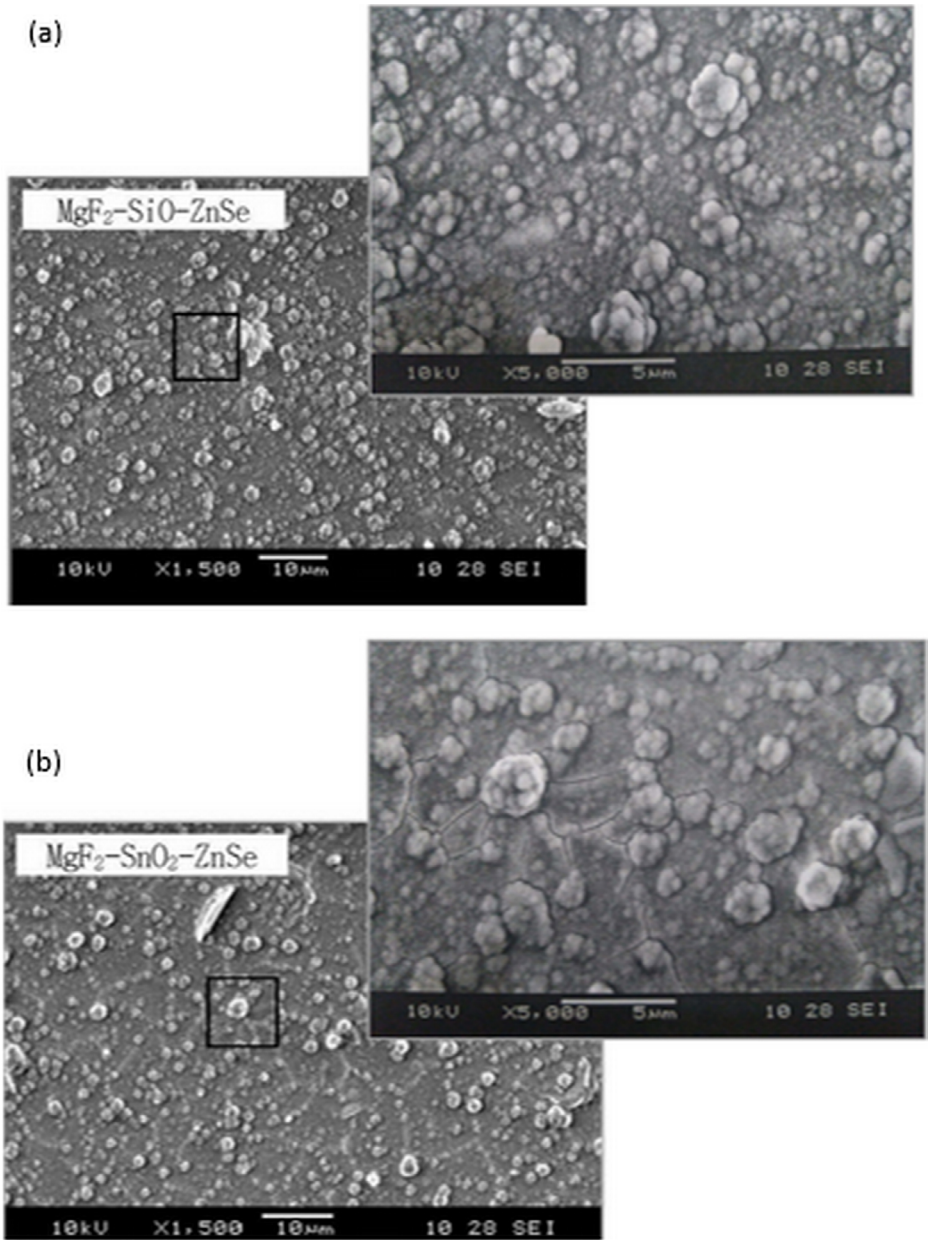

Figure 4. SEM micrographs showing the morphology of the experimental antireflection coatings. Insets are the higher magnifications (5000x) of the selected regions.

Generally, thin-films are under elastic stresses after deposition, whose magnitude determines the integrity and performance. The sources of the elastic stresses include external (σ_e), thermal (σ_φ), and intrinsic (σ_i) stresses[23]:

$$\sigma = \sigma_e + \sigma_\varphi + \sigma_i \quad (16)$$

The sources of external stress (σ_e) include any external impact, application of static or dynamic forces, etc., while thermal stresses (σ_φ) are induced by not only the deposition process but also caused by the thermal treatments or varying temperature conditions. Intrinsic stresses are originated through the microstructural features of the thin film, which could be influenced by the film growth rate, mechanism, microstructural interaction, and contaminants. In any particular case, intrinsic stresses could be the highest in magnitude and contribute dominantly towards the performance of the film[21].

In the present case, where surface cracks were found in MgF_2-SnO_2-ZnSe; the primary factor of the cracking could be the intrinsic stresses generated due to microstructural mismatch between the subsequent layers. However, the precise identification and determination of the stress values are beyond the scope of the work undertaken and might be carried out in a separate study. Nevertheless, the presence of surface cracks in the coating may result in spalling and degradation of antireflection characteristics by subsequent moisture absorption.

Figure 5 shows the superimposed experimental reflection spectra of the coatings. The experimental reflection of the lead sulfide is higher than the theoretical values and it also accompanies profile variations, which are more pronounced at higher wavelengths i.e., beyond 1850 nm. These variations in the reflection and profile could be due to the surface defects, surface morphology, and the film discontinuities. Similarly, the reflections of three-layer antireflection coatings followed the profile of the uncoated lead sulfide, however an appreciable decrease in reflection occurred after the coating i.e., 30%. In comparison, the antireflection coating of combination-I, where the sandwich layer is SiO, the overall reflection profile is lower than the combination-II (with SnO_2 as a sandwich layer). It could be due to the surface cracks in the combination-II coating, which may absorbed the moisture from the environment and caused a higher degree of the reflection, besides scattering of the incident radiations.

Albeit, the experimental reflectance spectra of the antireflection coatings showed a noticeable decrease in reflection as compared to the uncoated lead sulfide, however the spectra of the theoretical coatings were further lower. In case of MgF_2-SiO-ZnSe coating, the experimental reflectance spectrum was comparable with the theoretical curve between 1500 to 1800 nm, while in the region between 1800 to 2400 nm, the reflectance of experimental curve was higher than the theoretical one. The deviation could be attributed to the defects in the coatings and/or sensitivity of the coating to the small variations in the thickness; nevertheless, the deviation remained limited to 5-8 %.

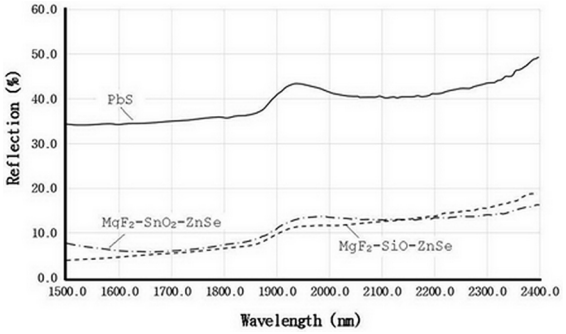

Figure 5. Superimposed reflection spectra of the experimentally coated thin films.

In the case of MgF_2-SnO_2-ZnSe coating, the deviation between theoretical and experimental spectra was even at higher side i.e. 6% in 1500 to 1800 nm region and ~16% in 1800 to 2400 nm region. The higher deviation of the experimental results from theoretical values could be due to the higher density of defects and cracks in the film, which in turn absorbs more moisture from the environment, hence influences the reflectance of the film.

5. Conclusions

Design and simulation of three- layer antireflection coating was successfully realized using an optical matrix approach for highly refractive lead sulfide thin film surfaces.

Both the coatings were analogous in morphology, however the MgF_2-SiO-ZnSe coating was crack free as compare to MgF_2-SnO_2-ZnSe coating.

The experimental reflection spectra revealed that a 30% reduction in reflectance was achievable for either combinations of three- layer antireflection coatings.

In comparison, the antireflection coating having SiO as sandwich layer, the overall reflection profile is lower than the coating with SnO_2 as sandwich layer.

The theoretical and experimental reflectance spectra were more comparable in case of MgF_2-SiO-ZnSe coating than MgF_2-SnO_2-ZnSe.

6. References

1. Thelen A. *Design of optical interference coatings*. Pennsylvania: McGraw-Hill; 1989.

2. Muhammad HA, Muhammad BK, Naseem S, Khan ZA. Design and preparation of antireflection films on glass substrate. *Turk Journal of Physics*. 2005;29:43-53.

3. Park SI, Lee YJ. Design of multilayer antirefection coatings. *Journal of the Korean Physical Society*. 1998;32:676-680.

4. Friz M, Waibel F. Coating materials. Merck KGaA, d-64579. Germany, Gernsheim: editora; 2015.

5. Mehdi KH, Mady E. Antireflective Coatings: Conventional Stacking Layers and Ultrathin Plasmonic Meta-surfaces, A Mini-Review. *Materials*. 2016;9(6):497-507.

6. Majid M, Morteza KA. Various Types of Anti-Reflective Coatings (Arcs) Based on the Layer Composition and Surface Topography: A Review. *Reviews in Advanced Materials Science*. 2018;53:187-205.

7. Van Der Groep J, Spinelli P, Polman A. Single-Step Soft-Imprinted Large-Area Nano-patterned Antireflection Coating. *Nano Letters*. 2015;15(6):4223-4228.

8. Li J, Lu Y, Lan P, Zhang X, Xu W, Tan R, et al. Design, preparation, and durability of TiO_2/SiO_2 and ZrO/SiO_2 double-layer antireflective coatings in crystalline silicon solar modules. *Solar Energy*. 2013;89:134-142.

9. Kats M, Blanchard R, Genevet P, Capasso F. Nanometre optical coatings based on strong interference effects in highly absorbing. *Nature Materials*. 2013;12(1):20-4.

10. Orfanidis SJ. Electromagnetic Waves and Antenna. Piscataway, NJ: ECE Department; 2016; [access in 2019 jun 12]. Available from: http://eceweb1.rutgers.edu/ ~{}orfanidi/ewa/

11. Zhang H, Hu X, Sun Y, Zheng Y, Yan L, Jiang B, et al. Design and sol-gel preparation of six-layer tri-wavelength ORMOSIL antireflective coating for high power laser system. *RSC Advance Materials*. 2016;6(38):31769-31774.

12. Jeong O, Lee A, Raum C, Suzuki A. Broadband plasma-sprayed anti-reflection coating for millimeter-wave astrophysics experiments. *Journal of Low Temperature Physics*. 2016;184(1-3):621-6.

13. Loh JYY, Puzzo DP, O'Brien PG, Ozin GA, Kherani NP. Enhancing photovoltaics with broadband high-transparency glass using porosity-tuned multilayer silica nanoparticle anti-reflective coatings. *RSC Advanced Materials*. 2014;4(59):31188-31195.

14. Szczyrbowski J, Bräuer G, Teschner G, Zmelty A. Antireflective coatings on large scale substrates produced by reactive twin-magnetron sputtering. *Journal of Non-Crystalline Solids*. 1997;218:25-29.

15. Mazur M, Wojcieszak D, Kaczmarek D, Domaradzki J, Song S, Gibson D, et al. Functional photocatalytically active and scratch resistant antireflective coating based on TiO_2 and SiO_2. *Applied Surface Science*. 2016;380:165-171.

16. Glös D, Frach P, Gottfried C, Klinkenberg S, Liebig JS, Hentsch W, et al. Multifunctional high-reflective and antireflective layer systems with easy-to-clean properties. *Thin Solid Films*. 2008;516(14):4487-4489.

17. Reddy GB, Pandya DK, Chopra KL. Chemically deposited PbS-antireflection layer selective absorbers. *Solar Energy Materials*. 1987;15(3):162-187.

18. Ali JM, Salim SGR, Muhammad MS, Marwa A, Muhsien H. Structural Characterization of Lead Sulfide Thin Films by means of FTIR Analysis after Irradiation of β-ray. *British Journal of Science*. 2012;7:35-37.

19. Selhofer HE, Ritter E, Linsbod R. Properties of titanium oxide films prepared by reactive electron beam evaporation from various starting materials. *Applied Optics*. 2002;41(4):756-762.

20. Bennet JM, Pelletier E, Albrand G, Borgogno JP, Lazarides B, Charles K, et al. Comparision of properties of titanium dioxide film prepared by various techniques. *Applied Optics*. 1998;28(16):3303-3317.

21. Xu L, He J. Antifogging and antireflection coatings fabricated by integrating solid and mesoporous silica nanoparticles without any post-treatments. *Applied Material and Interfaces*. 2012;4(6):3293-3299.

22. Macleod HA. *Thin film optical filters*. 3rd ed. Philadelphia: Institute of Physics Publishing; 2001.

23. Kaiser N, Pulker HK. *Optical Interference Coatings*. Berlin: Springer-Verlag; 2003.